A 2-AXIS SI/AL BIMORPH-BASED ELECTROTHERMAL MICROMIRROR INTEGRATED WITH PIEZORESISTORS FOR HIGH RESOLUTION POSITION SENSING

Yue Tang[1,2], Xiaoyi Wang[1,2], Lixin Xu[3], and Huikai Xie[1,2]
[1]School of Information and Electronics, Beijing Institute of Technology, Beijing, China
[2]BIT Chongqing Institute of Microelectronics and Microsystems, Chongqing, China and
[3]School of Mechatronical Engineering, Beijing Institute of Technology, Beijing, China

2024 IEEE 37th International Conference on Micro Electro Mechanical Systems (MEMS) | 979-8-3503-5792-9/24/$31.00 ©2024 IEEE | DOI: 10.1109/MEMS58180.2024.10439337

ABSTRACT

In this work, single-crystal silicon (SCS) is employed to replace fragile SiO_2 to construct robust 2-axis electrothermal micromirrors with piezoresistors for position sensing. A lateral shift-free (LSF) SCS/Al bimorph electrothermal bimorph actuator is proposed, and a two-axis LSF SCS/Al electrothermal micromirror with piezoresistors was designed, fabricated and characterized. Each actuator was composed of six segments of bimorph and a thin silicon layer with the thickness of 2 μm. The dimensions of the square mirror plate are 1800 μm × 1800 μm × 30 μm. The fabricated micromirror achieved a tip-tilt angle of 7.2 ° and piston displacement of 240 μm under a voltage of 5 V. The performance of the angular shift of the proposed micromirror was improved about one order of magnitude with the value decreasing from 0.035 ° under open-loop control to 0.0062 ° under closed-loop control. Compared with SiO_2-based bimorphs, the fabrication process is not only simplified, but also provides a method for integrating piezoresistive sensors on the bimorph actuator and realizing feedback control.

KEYWORDS

MEMS micromirror, electrothermal actuation, SCS/Al bimorph, angular shift, feedback control

INTRODUCTION

MEMS micromirrors are composed of micro-actuators and a reflector, which is a basic component in optics for manipulating and modulating optical beams. MEMS micromirrors have been successfully used in automotive industry, aerospace, medical imaging, projection [1]-[4], more specifically, MEMS LiDAR for self-driving cars, hyperspectral devices for remote sensing [5] and environment monitoring [6], optical coherence tomography (OCT) for cancer screening [7], and portable Fourier transfer spectrometers (FTS) for agriculture [8].

According to different actuation mechanisms, four types of MEMS micromirrors are researched widely, including electrostatic, electromagnetic, piezoelectric and electrothermal micromirrors [9]. Electrostatic micromirrors are actuated mainly by parallel plates or comb drives [10]-[12]. Electromagnetic micromirrors rely on coils and magnets [13]. Piezoelectric micromirrors are based on the inverse piezoelectric effect of piezoelectric materials [14]. Electrothermal micromirrors may utilize bimorph beams that are stacked by two materials with largely different coefficient of thermal expansion (CTE) [15]. Although compared to electrostatic, electromagnetic and piezoelectric micromirrors, electrothermal bimorph micromirrors are relatively slower, but they can realize larger piston displacement and larger tip-tilt angle with low driving voltage [9], which have been used for OCT medical imaging [7] and FTS for ingredient analysis of soybeans [8].

For an electrothermal bimorph actuator, the larger the CTE difference between the two materials, the higher the actuation responsivity is. Thus, traditionally electrothermal bimorphs are often based on SiO_2 and a metal, such as SiO_2/Al and SiO_2/Au [16]. However, thin-film SiO_2 is fragile compared with single crystal silicon (SCS), because SiO_2 has much lower fracture strength (about 600-900 MPa) [17] than SCS (about 6-7 GPa) [18]. Also, SiO_2/Al-based electrothermal micromirrors have to be operated under thermal conditions without feedback control due to the incompatible fabrication with silicon-based feedback sensors, which usually undermine the stability and repeatability of those devices. In order to increase the scan stability and control robustness of electrothermal micromirrors, a SCS/Al bimorph-based electrothermal micromirror integrated with piezoresistive angular sensors is proposed. The device design, fabrication and characterization are discussed below.

DESIGN AND METHOD

The proposed electrothermal micromirror is shown in Figure 1(a). The mirror plate coated with a thin Al layer was connected to four actuators through four Si_3N_4/SiO_2 connectors. The four actuators were denoted as Act-1, Act-2, Act-3 and Act-4, respectively. All four actuators owned the same structure and parameters for driving uniformity. In order to sense the angle or displacement of the mirror plate, each actuator and piezoresistor were both supported by a flexure extended from the frame, as illustrated in Figure 1(b). Each piezoresistive sensor consisted of four terminals, two for input and two for output.

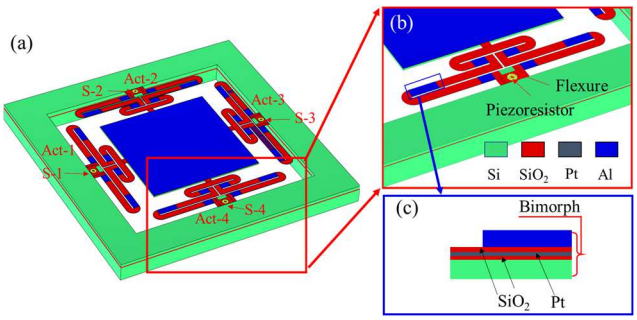

Figure 1: (a) Schematic of the electrothermal micromirror with Si-based bimorphs; (b) close-up of the actuator from side view; (c) close-up of the bimorph.

In order to eliminate the leakage current of the piezoresistive sensors, each sensor was insulated by a zone filled with Si_3N_4/SiO_2. The insulated zone can also decrease the thermal influence on the piezoresistors due to the low thermal conductivities of Si_3N_4 and SiO_2. The doped thickness of each sensor is about 800 nm. The thicknesses of the flexure and insulated zone both are 2 μm. The length and width of the sensor doping region both are 80 μm. Both of the length and width of the mirror plate are 1800 μm. The thickness of the mirror plate is about 30 μm to keep it with a good stiffness.

As shown in Figure 1(c), each bimorph is a stack of an SCS and an Al layer. Meanwhile, there are two thin SiO_2 layers and one thin platinum (Pt) layer between the SCS and Al layers, and the Pt layer is sandwiched between two SiO_2 layers, which plays the role as a heater.

In general, the bimorph is fixed at one side and heated, causing a deflection d_f on the free side, which can be expressed by the following equation [9]:

$$d_f = \frac{3L_b^2\left(t_{Al}+t_{Si}\right)\left(a_{Al}-a_{Si}\right)\Delta T}{\left(4t_{Si}^2+4t_{Al}^2+6t_{Si}t_{Al}+\frac{E_{Si}t_{Si}^3}{E_{Al}t_{Al}}+\frac{E_{Al}t_{Al}^3}{E_{Si}t_{Si}}\right)} \quad (1)$$

where, L_b is the length of the bimorph, t and α are the thickness and CTE of each material, respectively, E denotes the Young's module of each material, and ΔT is the temperature difference between the bimorph and ambient.

DEVICE FABRICATION

The process started with an SOI wafer with a 2 μm-thick device layer in N type, as shown in Figure 2(a). First, a 500 nm thick SiO_2 layer is deposited on the device layer by PECVD. Then the SiO_2 layer was patterned and etched before the first thermal diffusion. After spinning borofilm 100 solution on the top layer, the wafer was processed in a thermal annealing tube for the first thermal diffusion to form piezoresistive sensors. After that, the remained borofilm 100 solution and SiO_2 were removed by BOE solution. Then the second thermal diffusion was performed through repeating the former processes to form highly doped ohmic contact areas. Then, isolation grooves were etched by DRIE and filled with Si_3N_4/SiO_2 for thermal and electrical insulation. The connector between the actuators and mirror plate was simultaneously formed by filling Si_3N_4/SiO_2. Next, for MEMS micromirror fabrication, Pt, SiO_2 and Al layers were deposited on the top layer; then the top layer was etched again by DRIE to pattern actuators and the mirror plate. After completing all of the above steps, the cross section was as illustrated in Figure 2(b). Continually, a silicon step was formed on from the backside of the SOI wafer by DRIE, which was around 30 μm in height, as shown in Figure 2(c). After that, the photoresist was removed and the handle layer was etched until the buried oxide layer of the SOI was exposed. At last, the buried oxide layer was removed by vapor HF to release the device, as shown in Figure 2(d).

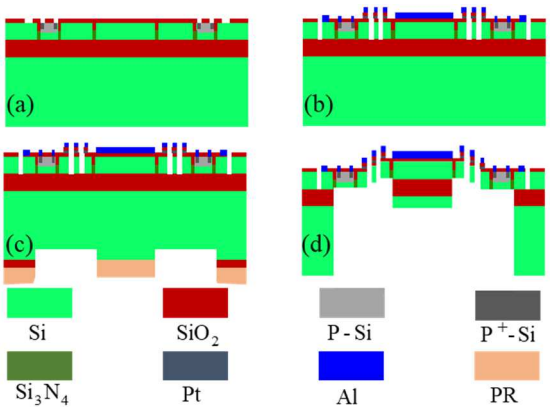

Figure 2: Schematics of the fabrication processes of the proposed electrothermal micromirror.

The device shown in Figure 3(a) is a final released micromirror, where the mirror plate is 1800 μm by 1800 μm. It is clear from the figure that the mirror plate is elevated due to the residual stresses in the bimorph beams. The elevation is 200 μm. SCS/Al Bimorphs are also shown in Figure 3(a). A close-up of a piezoresistive sensor is shown in Figure 3(b). The Si_3N_4/SiO_2 zone insulates the flexure from the actuator. The flexure potentially provides the area to integrate piezoresistive sensors for sensing the angle of the mirror plate.

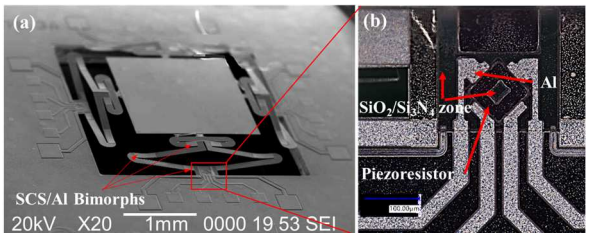

Figure 3: (a) SEM image of the proposed micromirror; (b) close-up of one of piezoresistors.

CHARACTERIZATIONS

A diagram of the setup for measuring the performance of the fabricated micromirror is shown in Figure 4. The incident beam from a laser is reflected into MEMS micromirror by a reflector, and the reflected beam from the micromirror is then received by a PSD. The PSD signals, which include X and Y locations, are amplified by an On-Trak PSD amplifier. The X and Y signals from the amplifier are processed by a computer. The MEMS micromirror is driven by a signal generator or DC voltage source. The static and dynamic characteristics of the MEMS micromirror can be obtained by this setup.

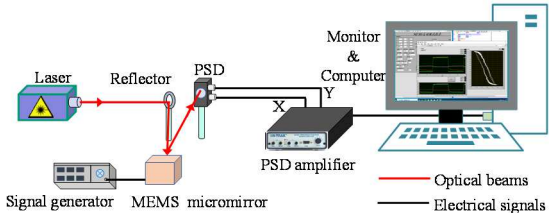

Figure 4: Schematic of the experimental setup.

Lissajous scanning

By applying two sinusoidal signals with the same amplitude and frequency, e.g., 4 V and 6 Hz, but a phase difference of 45°, an elliptical scanning pattern can be obtained, as shown in Figure 5(a). When these two signals have the same amplitude and phase with different frequencies, e.g., 10 Hz to Act-1 and 11 Hz to Act-2, a Lissajous pattern can be obtained, as shown in Figure 5(b).

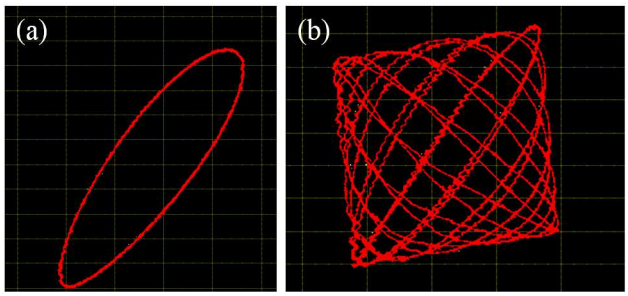

Figure 5: (a) Elliptical scanning; (b) Lissajous scanning.

Scanning angle and vertical displacement

As shown in Figure 6(a), the red line shows the simulation results using COMSOL Multiphysics and the black line shows the experimental results by driving Act-1. From the black curve, we can obtain that the largest optical scan angle is 7.2° under 5 V dc for the experiment, which is very close to the simulation result of 7.5°. The angle deviation between the test result and the simulation result is about 4.2% for the largest scan angle. The vertical displacement is achieved by applying the same DC voltage on all four actuators and the motion of the mirror plate is measured with an optical microscope. Under 5V DC signal, the vertical displacements are 240 μm for the experiment and 250 μm for the simulation, respectively.

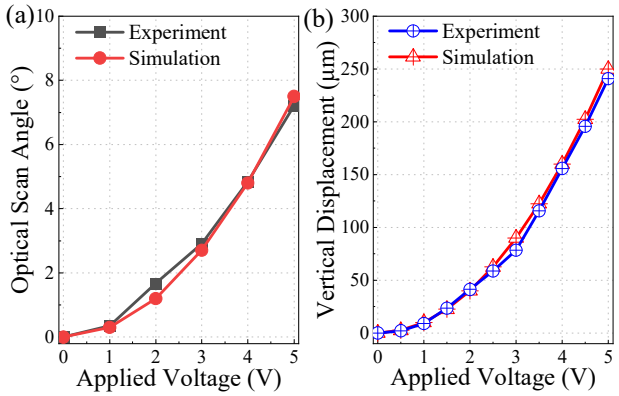

Figure 6: (a) Optical scan angle vs. applied voltage; (b) vertical displacement vs. applied voltage.

Step response

A step signal with an amplitude of 3 V and a frequency of 1 Hz is applied on one of the four actuators of the MEMS micromirror, and the synchronizing step signal and the PSD signal are acquired and sent to a computer. The step response result is shown in Figure 7. The blue line is the signal from the PSD and the red line is the step signal. The thermal response time is about 72 ms.

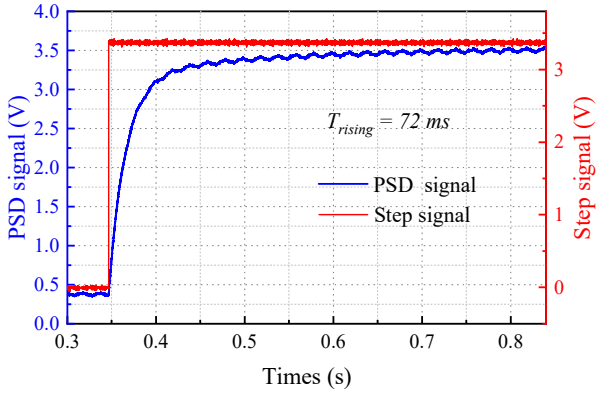

Figure 7: Step response of the proposed micromirror.

PID Control result

As shown in Figure 8, the angular drift is reduced from 0.035° under open loop control to 0.0062° under PID control, which means that this work is comparable with other works [19] [20] using large photodetectors (PDs) for closed-loop control, as shown in Table 1.

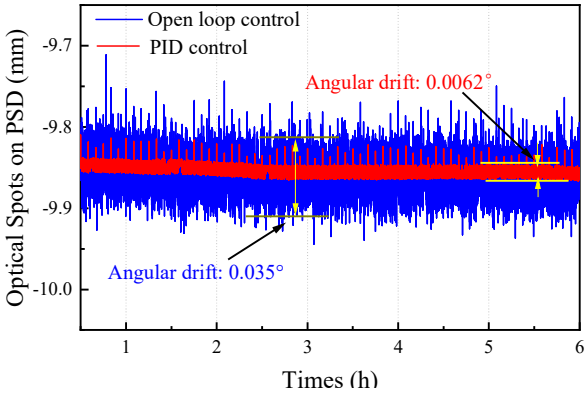

Figure 8: Open loop control vs. PID control.

Table 1: Compare with other works.

Reference	Feedback types	Angular drift (°)	Bimorph materials
this work	piezoresistors	0.0062	SCS/Al
[19]	VCSEL & PDs	0.0067	SiO_2/Al
[20]	large outer PD	0.0015	SiO_2/Al
[21]	no feedback	0.097	SiO_2/Al

CONCLUSION

In this paper, the design and fabrication of a SCS/Al bimorph-based 2-axis electrothermal micromirror integrated with angular sensors is reported. This new micromirror consists of LSF electrothermal actuators embedded with a 2 μm-thick SCS layer. A flexure is designed for integrating SCS-based piezoresistive sensors between the external frame and each actuator. Each angular sensor has four terminals and works based on pseudo hall effect. And each sensor is insulated by a Si_3N_4 and SiO_2 zone to decrease the leakage current and the heat flux from the actuator. Finally, the proposed electrothermal micromirror has a low angular shift under closed-loop control. More efforts will be focused on optimizing the design and fabrication process for the future work.

ACKNOWLEDGEMENTS

This work is supported by the National Natural Science Foundation of China under Grant# 6231101499.

REFERENCES

[1] H. Yoo, N. Drumal, et al., “MEMS-based lidar for autonomous driving”, *Elektrotech. Inftech*, vol. 135, pp. 408-415, 2018.

[2] B. Alvise, A. Sitar, er al., "High Frequency MEMS Capacitive Mirror for Space Applications", *Micromachines*, vol. 14, pp. 158, 2023.

[3] L. Xi, J. Sun, et al., "Photoacoustic imaging based on MEMS mirror scanning", *Biomed. Opt. Express*, vol. 1, pp. 1278-1283, 2010.

[4] C. -C. Tsai, Z. -H. Li, Y. -T. Lin and M. S. -C. Lu, "A Closed-Loop Controlled CMOS MEMS Biaxial Scanning Mirror for Projection Displays", *IEEE Sensors Journal*, vol. 20, no. 1, pp. 242-249, 2020.

[5] S. Bish, Y. Wang, J. W. Tunnell and X. Zhang, "MEMS scanner based handheld fluorescent hyperspectral imaging system", *2011 TRANSDUCERS*, Beijing, China, 2011, pp. 2542-2545.

[6] L. Li, C. Huang, H. Zhang, "Micro/Nanoscale Optical Devices for Hyperspectral Imaging System", *Outlook and Challenges of Nano Devic*es, *Sensors*, *and MEMS*, Springer Cham, pp. 459-482, 2017.

[7] H. Xie, J. Sun, S. Guo and L. Wu, "3D endoscopic optical coherence tomography based on rapid-scanning MEMS mirrors", *2009 Asia Communications and Photonics conference and Exhibition (ACP)*, Shanghai, China, 2009, pp. 1-6.

[8] D. Wang, P. Wang, et al., "Nondestructive On-Site Detection of Soybean Contents Based on An Electrothermal MEMS Fourier Transform Spectrometer," *IEEE Photonics Journal*, vol. 11, no. 3, pp. 1-10, June 2019.

[9] Y. Tang, J. Li, L. Xu, J.B. Lee, H. Xie, “Review of Electrothermal Micromirrors”, *Micromachines*, vol. 13, pp. 429, 2022.

[10] J. B. Sampsell, "Digital micromirror device and its application to projection displays", *Journal of Vacuum Science & Technology B: Microelectronics and Nanometer Structures Processing, Measurement, and Phenomena*, vol. 12, no. 6, pp. 3242-3246, 1994.

[11] F. Hu, J. Yao, C. Qiu, et al., “A MEMS micromirror driven by electrostatic force”, *Journal of Electrostatics*, vol. 68, no. 3, pp. 237-242, 2010.

[12] Y. Cao, P. Wang, J. Li, et al., “Temperature stability study of resonant angular scanning micromirrors with electrostatic comb-drive actuators”, *Sensors and Actuators A: Physical*, vol. 318, pp. 112525, 2021.

[13] J. -Y. Hwang, J. -U. Bu and C. -H. Ji, "Low Power Electromagnetic Scanning Micromirror for LiDAR System", *IEEE Sensors Journal*, vol. 21, no. 6, pp. 7358-7366, 15 March15, 2021.

[14] K. H. Koh, T. Kobayashi, et al., “Characterization of piezoelectric PZT beam actuators for driving 2D scanning micromirrors”, *Sensors and Actuators A: Physical*, vol. 162, no. 2, pp. 336-347, 2010.

[15] A. Jain, T. Xie, Y. Pan, G. K. Fedder and H. Xie, "A two-axis electrothermal SCS micromirror for biomedical imaging," *2003 IEEE/LEOS International Conference on Optical MEMS (Cat. No.03EX682)*, Waikoloa, HI, USA, 2003, pp. 14-15.

[16] A. Minhas, A. Kumar, et al., “Fabrication of electro-thermally driven tunable plate with Au/SiO_2 bimorph beams”, *Microsyst. Technol.*, vol. 25, pp. 2821-2829, 2019.

[17] V. Hatty, H. Kahn and A. H. Heuer, "Fracture Toughness, Fracture Strength, and Stress Corrosion Cracking of Silicon Dioxide Thin Films", *Journal of Microelectromechanical Systems*, vol. 17, no. 4, pp. 943-947, 2008.

[18] D. B. Heinz, I. B. Flader, et al., "Direct comparison of stiction properties of oxide coated polysilicon and smooth single crystal silicon", *2017 TRANSDUCERS*, Kaohsiung, Taiwan, 2017, pp. 1203-1206.

[19] Y. Liu, Y. Feng, et al., "Integrated tilt angle sensing for large displacement scanning MEMS mirrors", *Opt. Express*, vol. 26, pp. 25736-25749, 2018.

[20] F. Han, W. Wang, et la., "Miniature Fourier transform spectrometer with a dual closed-loop controlled electrothermal micromirror", *Opt. Express*, vol. 24, pp. 22650-22660, 2016.

[21] S. R. Samuelson and H. Xie, "A Large Piston Displacement MEMS Mirror With Electrothermal Ladder Actuator Arrays for Ultra-Low Tilt Applications", *Journal of Microelectromechanical Systems*, vol. 23, no. 1, pp. 39-49, Feb. 2014.

CONTACT

*H. Xie, tel: +86-10-68918442; hk.xie@ieee.org.